Seabed Classification From Multispectral Multibeam Data

Valsamis Ntouskos, Panagiotis Mertikas, Angelos Mallios, *Member, IEEE*, and Konstantinos Karantzalos, *Senior Member, IEEE*

***Abstract*—Given the recent increase in the availability of multispectral multibeam echosounder data, this work aims to identify suitable processing and classification methodologies for seabed classification based on such data. We propose a complete processing and classification pipeline and investigate the adequacy of state-of-the-art classification algorithms to perform seabed classification based on multispectral backscatter data alone, and when additional data sources are considered. Starting from raw acquisition data, we generate region-wide multispectral backscatter composite images through noise removal, inpainting/gap-filling and mosaicking. Ground truth data from in situ seabed samples are used. We have tried different classification methods, including random forests, support vector machines, and multilayer perceptrons, with the latter providing the best results. Quantitative and qualitative evaluation on five surveys indicate high classification performance based only on multispectral backscatter data, while additional features, like bathymetry, bathymetric positional index (BPI), or positional encoding, offer limited gains. We offer a web service for seabed classification from multispectral multibeam echosounder data to further support and increase interest in the topic.**

***Index Terms*—Backscatter, data analysis, echo sounding, machine learning, seabed classification, seafloor mapping.**

I. Introduction

THE ability to map the composition of the seabed is crucial across a wide range of applications in various sectors, including marine geology and biology, archaeology, energy, oil, and gas ([1], [2]). Different types of classification and categorization may be considered in terms of seabed classes depending on the application at hand ([3], [4]). Notwithstanding the major financial and scientific interest, seabed classification poses serious challenges due to a variety of factors [4]. These include the varying conditions in the water column that hinders remote sensing and inaccessibility which make sampling of ground truth data difficult and sparse.

The main means of collecting information about the seabed are echosounders, which emit sound pulses at specific frequencies and process their echoes. Compared to single-beam echo-sounders, multibeam echosounders (MBES) offer higher resolution and wider coverage because they use more receiver elements, allowing for beamforming. By analyzing the collected echoes, both the distance of the ensonified area from the sensor and its reflectivity characteristics can be estimated, producing bathymetric and backscatter data, respectively. The latter provide crucial information regarding the composition of the seabed. As a result, backscatter data have been considered as the primary feature for classifying and characterizing the seabed of a surveyed area ([5], [6], [7], [8], [9], [10]).

MBES typically operate at a single frequency, making interpretation and classification based on backscatter data challenging as different compositions can have similar responses at the used frequency, thus, requiring the integration of other data modalities like bathymetry and bathymetry-derived products to help the classification process [9], [10], [11]. Multispectral multibeam echosounder (MS-MBES) data can be collected either by performing multiple passes over the same area, by combining multiple units operating at different frequencies, or by using recently developed multifrequency echosounders. According to multispectral data collected from optical sensors, different sediment types and materials have different acoustic backscatter responses according to the frequency utilized, giving rise to distinct acoustic spectral signatures, thus, providing crucial information regarding the composition of the seabed ([12], [13], [14]).

Due to the relatively recent emergence of MS-MBES acquisition methods and their limited availability, only a few works have tackled the problem of seabed classification from multispectral backscatter data ([3], [14], [15], [16], [17]). Most of these methods have been proposed in the context of the R2Sonic Multispectral Challenge [18], which released a number of MS-MBES data sets acquired in the regions of Bedford Basin (CA), Patricia Bay (CA), and Lower Portsmouth (US) to explore new ways of using multispectral backscatter data for seabed classification

Manuscript received 21 September 2021; revised 24 February 2022 and 22 November 2022; accepted 11 April 2023. Date of publication 13 June 2023; date of current version 14 July 2023. This work was supported in part by Greece and the European Union European Social Fund through the Operational Programme "Human Resources Development, Education and Lifelong Learning" in the context of the project "Reinforcement of Postdoctoral Researchers - 2nd Cycle" under Grant MIS-5033021, implemented by the State Scholarships Foundation, in part by the SANTORY program funded by the Hellenic Foundation for Research and Innovation under Grant 1850, in part by the iSEAu EU H2020 MSCA project under Grant 101030367, and in part by the NEANIAS EU H2020 project under Grant 863448. *(Corresponding author: Valsamis Ntouskos.)*

Associate Editor: D. Simons.

Valsamis Ntouskos and Panagiotis Mertikas are with the Remote Sensing Laboratory, National Technical University of Athens, 15780 Zographos, Greece (e-mail: ntouskos@mail.ntua.gr; panag.mertikas@gmail.com).

Angelos Mallios is with the Ploa Technology Consultants S.L., Carrer Pic De Peguera 11 Parc Cientific I Tecnolgi Giroemprem A1-11, 17003 Girona, Spain (e-mail: amallios@ploatech.com).

Konstantinos Karantzalos is with the Remote Sensing Laboratory, National Technical University of Athens, 15780 Zographos, Greece, and also with the Research, Innovation Center in Information, Communication, Knowledge Technologies "Athena," 15125 Marousi, Greece (e-mail: karank@central.ntua.gr).

Digital Object Identifier 10.1109/JOE.2023.3267795

and characterization. Each method follows a different approach on how survey data are treated, how multispectral classes are defined, how sediment samples are considered, and what techniques are used for producing seabed classification maps.

In this work, we aim to simplify the process of seabed classification from MS-MBES data by exploiting prior knowledge in multispectral image classification, and improve the classification performance by employing state-of-the-art machine learning methods. Our evaluation uses the five data sets made available through the R2Sonic Multispectral Challenge [18], captured at three frequencies, namely, 100, 200, and 400 kHz (more details are provided in Section IV).

The contributions of this work are the following:

1) propose a complete processing pipeline for producing multispectral backscatter images of the seabed starting from the survey data. The pipeline considers removal of noisy areas, missing values completion via inpainting/gap-filling and composition of multichannel color composite images;
2) comprehensively evaluate seabed classification on the R2Sonic Multispectral Challenge data sets using three standard classifiers, Random Forests (RF), multilayer perceptron (MLP), and support vector machines (SVM), considering per region classification models, model transferability, and a comprehensive ablative study;
3) propose the use of positional encoding for encouraging local coherence of the resulting classification map;
4) through the evaluation show that MLPs perform better with respect to the other methods, while for all methods high classification performance can be achieved using MS-MBES data alone, with additional features (e.g., bathmetry and BPI) offering limited gains;
5) provide an on-line service for seabed classification based on MS-MBES data for reproducibility and for fostering further research on MS-MBES seabed classification methods.

The rest of this article is organized as follows. Section II discusses previous work, and Section III presents the proposed method for seabed classification from MS-MBES data. Section IV presents the data sets considered and discusses the experimental evaluation of the proposed method and Section V the corresponding web service, while Section VI concludes this article.

II. Related Work

A number of classification methods based on MBES data have been developed in the last decades to characterize the seabed, considering both single and multifrequency backscatter data, bathymetry, and other data sources ([3], [5], [6], [7], [8], [14], [15], [16], [17], [19]). Acoustic backscatter intensity together with bathymetry and bathymetry derived products, like slope, bathymetric position index (BPI) [20], etc., are the most common features used in seabed classification. Backscatter depends on the composition of the seabed, the angle of incidence, and the acoustic frequency [9], [10], [11], [21]. In several lab and field experiments, in which the influence of varying frequencies on the backscatter strength has been studied, it was shown that specific sediment types have different acoustic responses at different frequencies ([14], [15], [19], [21]). In this work, we explore the possibility that multispectral bacskcatter data are sufficient to perform accurate seabed classification, without the addition of other common data sources.

The following works used the R2Sonic Multispectral Challenge data sets [18]. In [15], the produced classification maps were based on the Bayesian method for sediment classification by using either single (100, 200, and 400 kHz) or multiple frequencies. Considering the MBES data set acquired in 2017 at Bedford Basin, single frequency backscatter data at 200 and 400 kHz suggested for a maximum of five acoustic classes each, while the multispectral approach resulted in a classification map consisting of nine multispectral acoustic classes. The evaluation of these methods was based on the spatial correlation of the acoustic classes derived within each frequency and the grab samples.

The method of [16] is based on conditional random field (CRF) and Gaussian mixture models (GMM) which were applied on the multispectral data acquired at Patricia Bay and Bedford Basin regions. The highest level of mean cross validation accuracy was 91% using four classes for Patricia Bay and 99.5% with three classes for Bedford Basin. For both experiments, the training data set was 50% of the seabed observations.

The approach of [3] used spatial patterns and in particular variable size cell (VSC) database architecture developed by Geoconsulting Marine of Halifax, Nova Scotia. This method has been applied on three MBES data sets, namely, Patricia Bay, Bedford Basin 2016 and 2017 and led to three classification maps respectively depicting nine seabed classes.

Finally, [17] used Boosted Regression and Classification Trees. Considering the MBES data sets of Bedford Basin 2016 and 2017 combined, they characterized three substrate and biological cover types with an average accuracy of 96%, with respect to reference sites where underwater photographs were available.

III. Multispectral Backscatter Processing and Classification

In this section, we present a complete MS-MBES data processing pipeline for seabed classification and characterization. The pipeline for producing seabed classification maps based on multispectral images, starting from GSF files containing data for individual scanlines, is summarized in Fig. 1.

A. Data Processing

We define first the preliminary processing steps utilized for converting the MS-MBES data sets from their raw data format to georeferenced multichannel raster data, which are used to produce highly accurate seabed classification maps for each study site [22]. The main processing steps are the following: 1) preprocessing and extraction of survey line data from raw survey data; 2) inpainting of noisy segments per survey line; 3) composition of multispectral raster images; 4) multispectral image normalization.

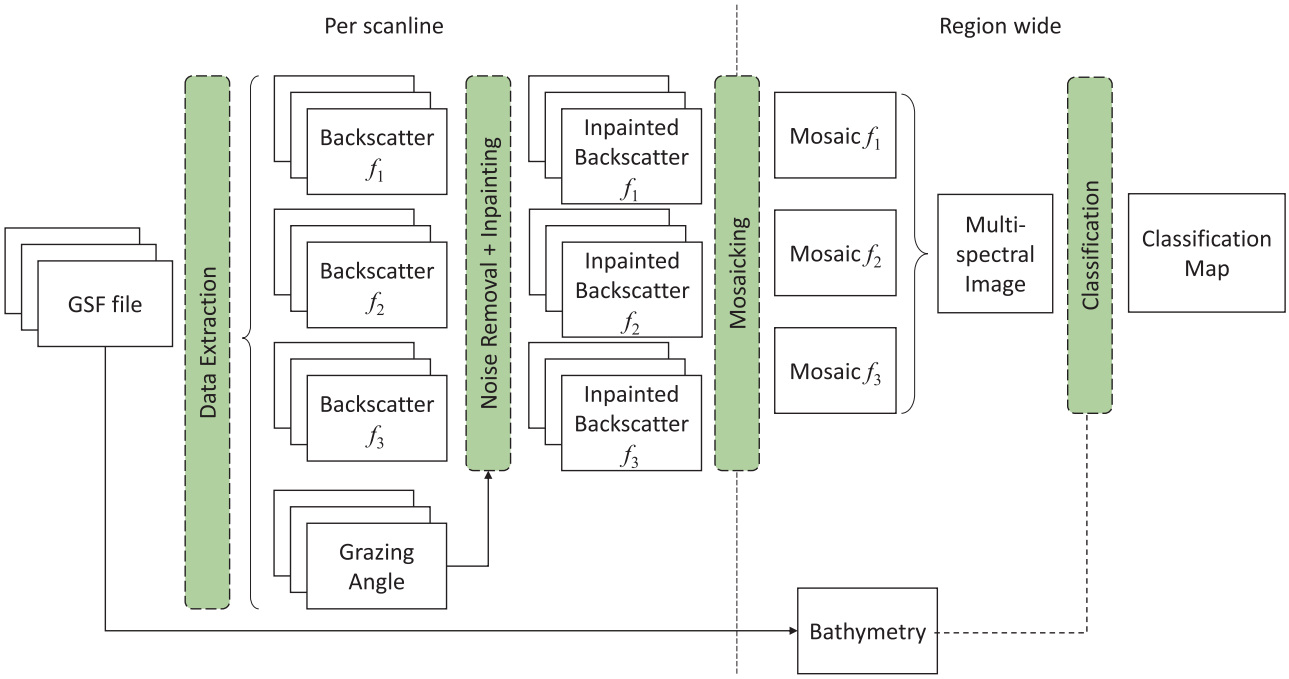

Fig. 1. Developed seabed classification methodology; starting from GSF multispectral multibeam data to the produced seafloor classification map for three frequencies (f_1, f_2, and f_3).

1) Preprocessing and Extraction of Survey Line Data: The first step is the preprocessing and extraction of the bathymetric and backscatter data of the MS-MBES surveys from the GSF files. First, all GSF files corresponding to a survey were imported to the MB-System open-source software ([23], [24], [25]) for initial processing. Both bathymetric and backscatter information are extracted from the survey data. Regarding bathymetry, rasters have been produced with a spatial resolution of 0.20 m based on all the data acquisition frequencies.

Regarding backscatter data, based on the additional data provided in the raw data files, all necessary corrections have been applied ([1], [4], [26], [27]). Data were processed separately for each acquisition frequency, namely, 100, 200, and 400 kHz, and Georeferenced rasters were produced for each survey line, considering the same spatial resolution as the bathymetry raster (0.20 m). The backscatter data had speckle in an area within $\pm 12^\circ$ from the nadir (approximately 7% of total swath) [27], as shown in Fig. 2. As this type of noise correlates with the beams' grazing angle, we have removed the data within a grazing angle of $\pm 12^\circ$.

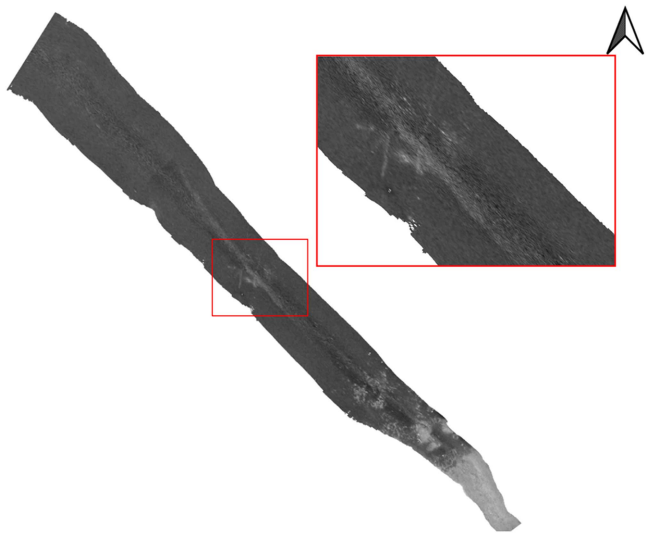

Fig. 2. Detail of noisy area of a survey line in the backscatter data.

2) Inpainting of Noisy Areas: After removing the noisy area from each survey line, gaps may remain in the mosaic even after combining all the survey lines, as shown in Fig. 3, despite the fact that the overlap between successive survey lines is typically close to 50%.

To obtain a gap-free mosaic, gaps in each survey line are filled via inpainting/gap-filling. Inpainting techniques aim to fill missing pixels in an image realistically, following the available context ([28], [29], [30]). We tried a range of method including [29], [30], and the angular dependence removal method of MB-System, however, they all produced unsatisfying results, with oversmoothed areas, and/or artefacts. Results from fast marching inpainting (FMI) [28] were more satisfying, as they followed better the distribution of the values surrounding the affected areas.

FMI starts from the boundary of the segment to be filled and proceeds to the inside. Each pixel to be inpainted is replaced by the normalized weighted sum of all the pixels with valid values in the neighborhood. The process is influenced heavily by the weights. Thus, more weight is given to the pixels close to the pixel being inpainted, close to the normal of the gap boundary and the pixels lying on boundary contours. Once a pixel is inpainted, the method moves to the nearest pixel using the fast marching method. FMI ensures that missing values close to known pixels are inpainted first, simulating a manual heuristic operation. An example of inpainting is presented on Fig. 4.

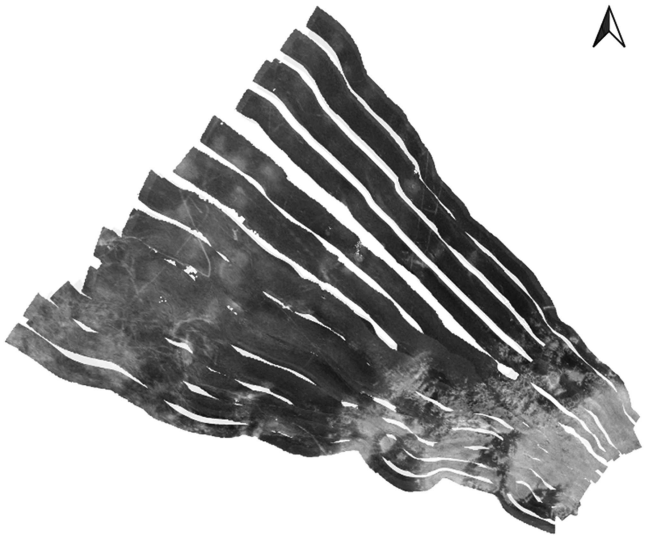

Fig. 3. Backscatter mosaic from multiple survey lines at 100 kHz from Bedford Basin 2016 after noise removal. Note that there are missing areas in the mosaic even though the overlap is close to 50%.

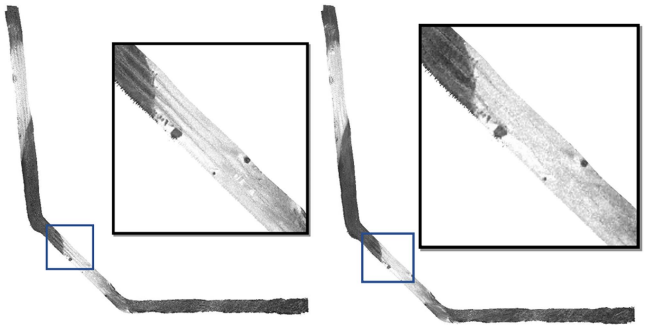

Fig. 4. Backscatter data mosaic at 100 kHz from the Lower Portsmouth Harbor before noise removal (left), and after removal and inpainting of the noisy area (right).

The above technique has been applied to each frequency separately for each survey line of a data set. After inpainting the noisy areas of each scanline, a mosaic is produced for all the survey lines of each frequency. These mosaics (here, for 100, 200, and 400 kHz frequencies) are then combined producing a georeferenced color composite image.

3) Normalization of Multispectral Images: To reduce bias introduced during backscatter raster generation, on one hand, and increase numerical stability of the classification methods, on the other, we normalize each channel of the multispectral raster data corresponding to a specific data acquisition frequency. We applied standardization, where the mean intensity value of the channel is subtracted and the difference is divided by the variance of the values. Specifically, letting Ω denote the image domain, $\mathcal{N}$ the set of no-data locations, $\setminus$ the set difference operator, and I_{ijc} be the value of the multispectral image I at $(i, j) \in [0, 1]^{\Omega}$ and $c \in F$ with F the set of the image channels

$$I_{ijc}^{std} = \frac{I_{ijc} - \mu_c}{\sigma_c^2} \tag{1}$$

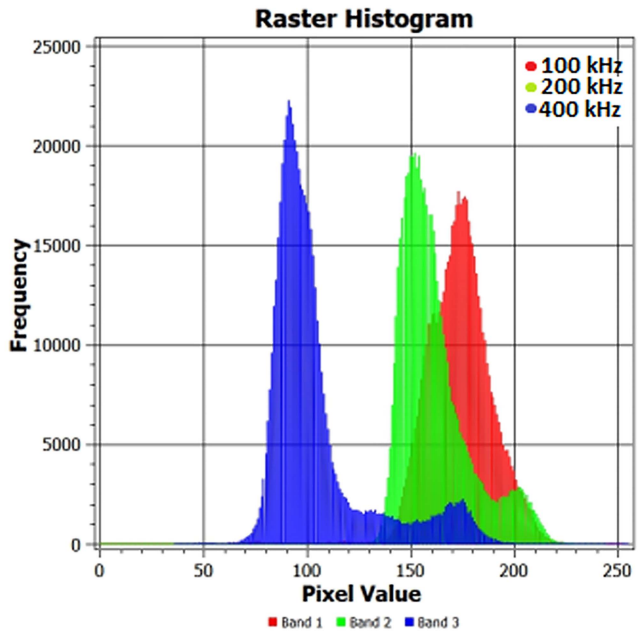

Fig. 5. Histogram of multispectral mosaic of Bedford Basin in 2017 before and after normalization. In particular, top: No normalization, and bottom: Std. Normalization.

with

$$\mu_c = \frac{\sum_{i,j \in \Omega \setminus \mathcal{N}} I_{ijc}}{|\Omega \setminus \mathcal{N}|}, \quad \sigma_c^2 = \frac{\sum_{i,j \in \Omega \setminus \mathcal{N}} (I_{ijc} - \mu_c)^2}{|\Omega \setminus \mathcal{N}|}. \tag{2}$$

We note here that to avoid leakage of information from training to validation/test data, normalization parameters (μ_c and σ_c) are computed based solely on the subset of data constituting the training set. An example of Bedford Basin 2017 survey histograms, before and after the standardization, is shown in Fig. 5.

B. Seabed Classification

1) Classification Models: We compute seabed classification maps by performing classification based on the generated multispectral images of the seabed. In particular, three main classification models were considered, namely, RF [31], MLP with two hidden layers [32], and linear SVM [33]. The intensity values (after normalization) of all frequency channels are provided as input to the models, which are trained to predict the corresponding seabed class.

We build ground truth data considering that pixels within a given radius from an in situ sample belong to the same seabed class as the sample. Additionally, to avoid spatial autocorrelation ([11], [34], [35]), we considered the annotated pixels to be grouped together based on the corresponding sample's ID. Then, to produce spatially disjoint training and validation sets, we perform splitting based on these IDs, ensuring that the resulting sets contain data from different samples. The training set is used to train the classification model and the validation set is used to evaluate the performance of the model. The classification models are compared based on their performance in Section IV, considering different splitting ratios.

Besides training classification models for each region separately, we examine how well the results of a model trained on the data of a specific survey can be transferred to a different survey, without retraining the model.

2) Additional Information: We also examine additional information that can be used to further increase the accuracy of the classification models. The most prominent is the bathymetry of the region as well as the BPI, which can be obtained from the survey data.

We also consider augmenting the input data with positional encoding to increase spatial coherence of the classification results. Positional encoding [36] captures the information regarding the relative position of a data sample with respect to the rest. Letting $X \in \mathbb{R}^{d\times N}$ the input data with d the encoding dimension and N the number of samples, $\mathbf{u} \in \mathbb{R}^{2\times N}$ denotes the 2-D image coordinates of the input data and σ a base encoding frequency, we can enrich the data with positional encoding as follows:

$$X^{PE} = X + \cos(2\pi B\mathbf{u}) + \sin(2\pi B\mathbf{u}) \tag{3}$$

with $B \in \mathbb{R}^{d\times 2}$ where each value is sampled from $\mathcal{N}(0, \sigma^2)$. The value of σ affects the degree of spatial coherence of the resulting classification map [37]. A suitable value can be found with a hyperparameter sweep.

Recently, positional encoding has gained a lot of attention due to its central role in Transformer networks [36], as well as its use in reconstructing high-frequency signals using MLPs [37]. Though typically used in the context of neural networks, positional encoding can assume analogous functionality when used with other machine learning models. Hence, here, we apply it to all types of models considered.

IV. Experimental Evaluation

In this section, we provide a comprehensive evaluation of the proposed seabed classification method based on multispectral images of the seabed. First, the data sets considered are described and, then, results of the quantitative and qualitative evaluation are provided. The quantitative evaluation is based on the standard metrics of Overall Accuracy (OA), User's Accuracy (UA), Producer's Accuracy (PA), and F1-score. Model transferability is also evaluated.

Moreover, an ablative study is presented assessing how different models, input data types and splitting ratios affect the results. Based on these results, MLPs have shown improved performance with respect to RFs and SVMs across all metrics considered. For this reason, MLPs with two hidden layers of 512 units are used as the reference classification model in this section.

TABLE I
Details of Surveys Considered

Region	Survey year	Format	# Survey Lines	Area (km^2)
Bedford Basin	2016	GSF	14	1.84
Bedford Basin	2017	GSF	13	2.30
Bedford Basin	2018	Raster	-	1.84
Patricia Bay	2016	GSF	8	0.84
Portsmouth	2017	GSF	9	0.50

TABLE II
Seabed Classes Considered According to EMODnet FOLK 5 Taxonomy

FOLK 5 based
Mud
Sand
mixed sediment
coarse sediment

A. Data Sets

Currently, public availability of MS-MBES data is rather limited. Hence, we base the evaluation of our method on the five MS-MBES survey data sets corresponding to three distinct regions provided in the context of the R2Sonic Multispectral Challenge 2017, captured with the R2Sonic 2026 Echosounder in three frequencies, namely 100, 200, and 400 kHz. Further details of the data sets considered are provided in Table I.

For the aforementioned regions the data that have been provided and utilized were either GSF files [38] or, in the case of Bedford Basin 2018, georeferenced multispectral images, as well as reference data and survey reports providing sediment classification information for each region. Ground truth data are taken within a given radius around available in situ samples. The classes considered follow the EMODnet FOLK taxonomy for five seabed classes [39]. Table II reports all the classes encountered in the data sets considered.

In the following, we discuss in detail the data considered for each region. Bathymetric and backscatter information, presented in the form of color composite images, for all regions is shown in Fig. 6.

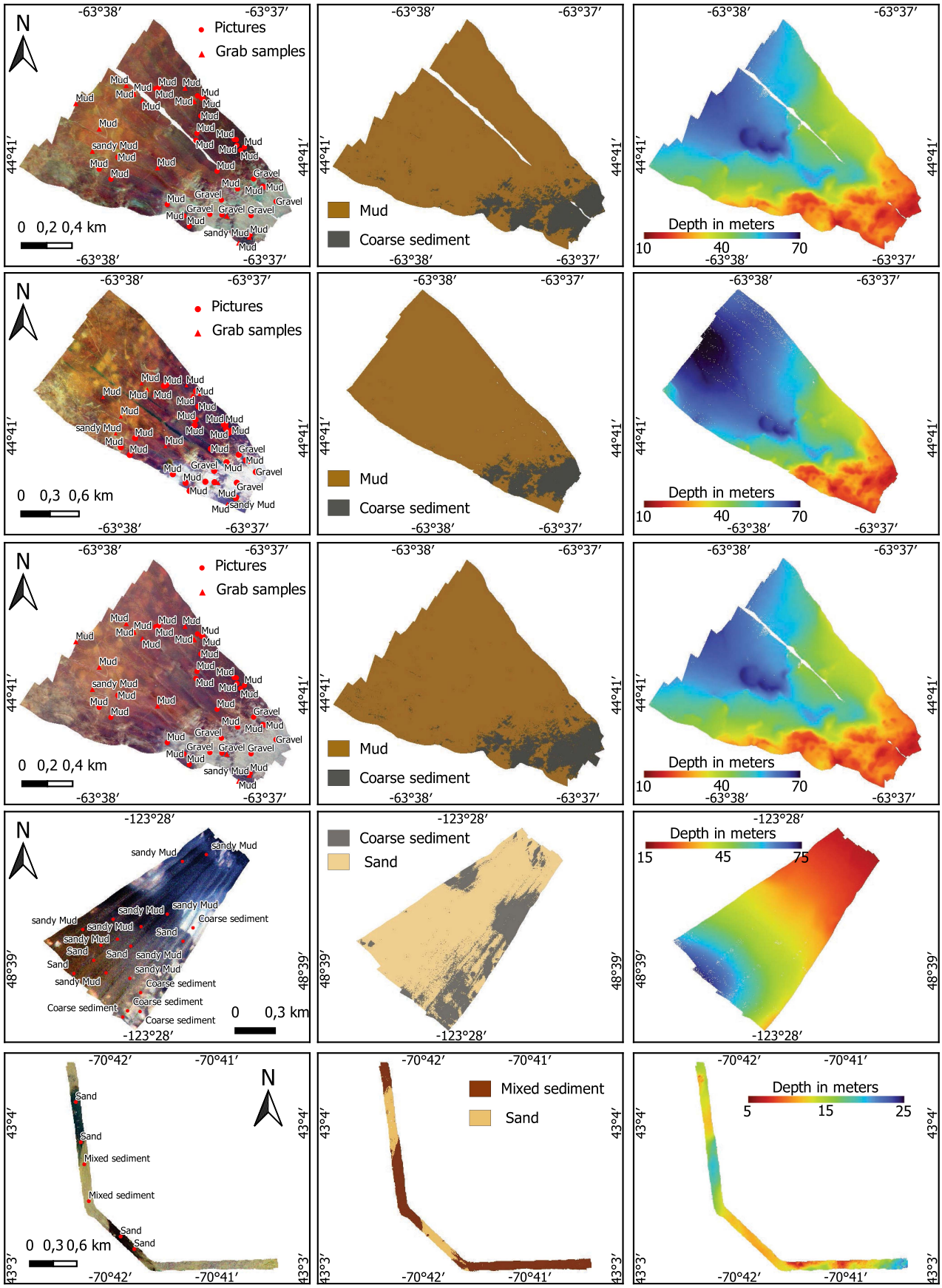

Fig. 6. Backscatter color composite images (1st column), classification results (2nd col.) and bathymetries (3rd col.) for the Bedford Basin 2016, 2017, 2018 (rows 1–3), Patricia Bay (4th row), and Lower Portsmouth (5th row) surveys.

TABLE III
CONFUSION MATRICES OF BEDFORD BASIN SEABED CLASSIFICATION FOR THE 2016 (LEFT), 2017 (MIDDLE), AND 2018 (RIGHT) SURVEYS USING MLP CLASSIFIER (ROWS CORRESPOND TO TRUE LABELS AND COLUMNS TO PREDICTED)

	Bedford Basin 2016				Bedford Basin 2017				Bedford Basin 2018			
	Mud	Coarse sediment	sum	PA	Mud	Coarse sediment	sum	PA	Mud	Coarse sediment	sum	PA
Mud	12120 (91.0%)	168 (1.3%)	12288	98.6%	14456 (88.8%)	805 (4.9%)	15261	94.7%	10774 (87.7%)	490 (4.0%)	11264	95.7%
Coarse sediment	0	1024 (7.7%)	1024	100.0%	0	1024 (6.3%)	1024	100.0%	0	1024 (8.3%)	1024	100.0%
sum	12120	1192	F1:	95.9%	14456	1829	F1:	84.5%	10774	1514	F1:	89.2%
UA	100.0%	85.9%	OA:	98.7%	100.0%	56.0%	OA:	95.1%	100.0%	67.6%	OA:	96.0%

Bedford Basin, Halifax NS, Canada: Three MS-MBES data sets have been acquired in Bedford Basin, Halifax, Nova Scotia in April 2016, May 2017, and December 2018, respectively, with the R2Sonic 2026 Multibeam Echosounder. The first two surveys, performed in 2016 and 2017, consist of 15[1] and 13 survey lines, respectively, with an approximate coverage of 1.84 and 2.30 km^2. Bathymetric maps of the surveyed sites, have been extracted from the provided GSF files, with the deepest area approaching 71 m. Regarding the MS-MBES data set of 2018, this has been provided as a multispectral mosaic along with the corresponding bathymetry and not in the form of individual survey lines.

Reference data: Ground truth consists of in situ seabed samples and pictures of the Bedford Basin region collected during the surveys.

Based on the analysis of these data, the following seabed classes have been identified for the Bedford region: 1) mud, and 2) coarse sediment. Two of the samples are of class "mixed sediment" (sandy mud) but they were not considered as they are insufficient for classification purposes.

Patricia Bay, North Saanich BC, Canada: The fourth survey corresponds to Patricia Bay, Canada and has been performed in November 2016, consisting of eight survey lines in total and a coverage area of 0.84 km^2. The water depth ranges from 25 to 75 m. According to [40] and [41], several distinct seabed types have been classified ranging from rock to mud over a wide range of depths in the bay.

Reference data: For the MS-MBES data set of Patricia Bay samples from the seabed were not directly available. Instead, we reused the seabed sample information reported in [40] based on a survey from 2005 performed with the Kongsberg Simrad EM300 echosounder. Specifically, ground-truth consists of point samples whose location is based on the map of [40] (after georeferencing), and whose classes are taken directly from the FOLK-like sample characterization as reported on the map. Based on these data, the seabed classes considered for the Patricia Bay region are: 1) sand, and 2) coarse sediment.

Portsmouth Harbor, NH, USA: The last survey has been conducted in the Portsmouth Harbor, New Hampshire, USA, with nine survey lines with a total covering area of approximately 0.5 km^2. Seabed backscatter observations at 100, 200, and 400 kHz were collected as the vessel made passage through the mouth of Portsmouth Harbor in water depths ranging from 5 to 25 m. Strong tidal currents, periodic storm waves, and a heterogeneous seafloor compose the area and a range of sediments from muddy fine sands to pebble and cobble gravels and bedrock outcrops ([42], [43]).

Reference data: As in the case of Patricia Bay, samples collected in a previous survey were used. In particular, ground truth data were based on a preceding survey performed with a singlebeam Simrad ES200-7CD SBES in 2013 [42] where seafloor imagery was also captured. Based on the grain size analysis provided in [42] for the samples collected in six sites, the classes considered are: 1) sand; and 2) mixed sediment.

B. Intraregion Classification

We first consider seabed classification maps obtained by training a classification model separately for each region. For each region, the reference data were taken within a radius of 4 m around the in situ samples and the were subsequently split randomly according to the sample ID taking 70% as training and 30% as validation data. To account for randomization effects, each experiment is performed three times and the average value from these runs is reported. Training of MLPs is performed on the training set and classification maps are generated by predicting the labels of the entire multispectral image (except nonvalid areas). Quantitative evaluation is performed on the validation set.

Fig. 6 presents the classification map obtained for each region, along with the color composite backscatter image and the bathymetry of the region, while Tables III and IV present the corresponding confusion matrices. We observe that in all cases classification accuracy is above 95%, while F1-score is higher than 84%. Qualitative assessment, suggests that classification results are in good agreement with the corresponding backscatter images. In particular, in the case of Patricia Bay, the classification map obtained is in good agreement with the classification map provided in [40], as can be seen in Fig. 7.

C. Model Transferability

We examine now the ability to use a model trained on the data of a specific survey to produce a classification map for a different survey. In particular, we examine the case of Bedford Basin surveys, taking all the labeled pixels of a specific survey/year for training and using the trained model to produce classification

[1]One survey line had to be discarded due to data conversion problems to the GSF format.

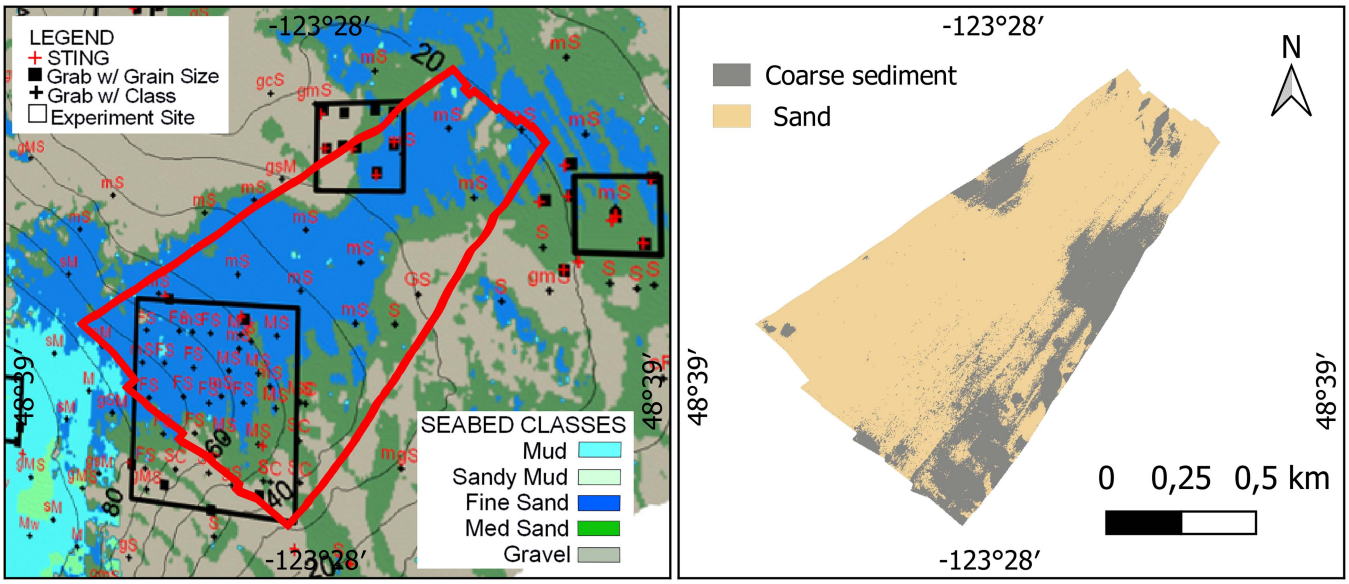

Fig. 7. Comparison of Patricia Bay Seabed Classification Map (right) with the aligned classification map provided in [40] (left).

TABLE IV
CONFUSION MATRIX FOR PATRICIA BAY 2016 SURVEY (TOP) AND LOWER PORTSMOUTH HARBOR 2017 SURVEY (BOTTOM) USING MLP CLASSIFIER (ROWS CORRESPOND TO TRUE LABELS AND COLUMNS TO PREDICTED)

	Patricia Bay 2016			
	Sand	Coarse sediment	sum	PA
Sand	4096 (80.0%)	0	4096	100%
Coarse sediment	0	1024 (20.0%)	1024	100%
sum	4096	1024	F1:	100%
UA	100%	100%	OA:	100%

	Lower Portsmouth Harbor 2017			
	Sand	Coarse sediment	sum	PA
Sand	1024 (50%)	0	1024	100%
Mixed sediment	0	1024 (50%)	1024	100%
sum	1024	1024	F1:	100%
UA	100%	100%	OA:	100%

maps of the remaining two surveys. It should be noted that as these three regions share the same sample points, we fix the IDs of the samples that act as training set and those that act as validation set. Training is performed on all train samples of the source region, and evaluation on all validation samples of the target region. Table V presents the evaluation results for all possible combinations. We see that the classification accuracy is above 80% in all cases while F1 scores are in the range of 62% to 88%.

TABLE V
MODEL TRANSFERABILITY ASSESSMENT ON THE BEDFORD REGION USING MLP MODELS (ROWS INDICATE THE TRAINING DATA SET AND COLUMNS THE EVALUATION DATA SET

	Bedford 2016		Bedford 2017		Bedford 2018	
	OA (%)	F1 (%)	OA (%)	F1 (%)	OA (%)	F1 (%)
Beford 2016	-	-	94.4	79.9	88.7	61.9
Beford 2017	86.8	79.1	-	-	92.9	81.2
Beford 2018	79.8	71.6	95.5	87.9	-	-

Table VI presents the confusion matrices when training is performed on the 2018 survey data (most recent) and evaluation on the 2016 and 2017 survey data. Fig. 8 presents the corresponding classification maps. We note that in the 2016 results most errors regard the misclassification of some muddy areas as coarse sediment ones.

D. Ablative Study

A comprehensive ablative study has been performed considering various aspects of the seabed classification method based on the MS-MBES data sets presented. In all cases, to account for randomization effects, we report the average of three consecutive runs. Moreover, to guarantee fair comparisons and repeatability, random seeds are fixed.

First, we examine the performance of the three types of classifiers considered, namely the Random Forest, multilayer perceptron, and the linear support vector machine classifiers, across all available regions and surveys by using 70% of the samples as training data set. Additionally, we study how the classification performance is affected by considering bathymetry, BPI and positional encoding[2] as additional data. The results are provided in Table VII, while the corresponding classification maps for the

[2]parameters σ are selected with hyperparameter sweep

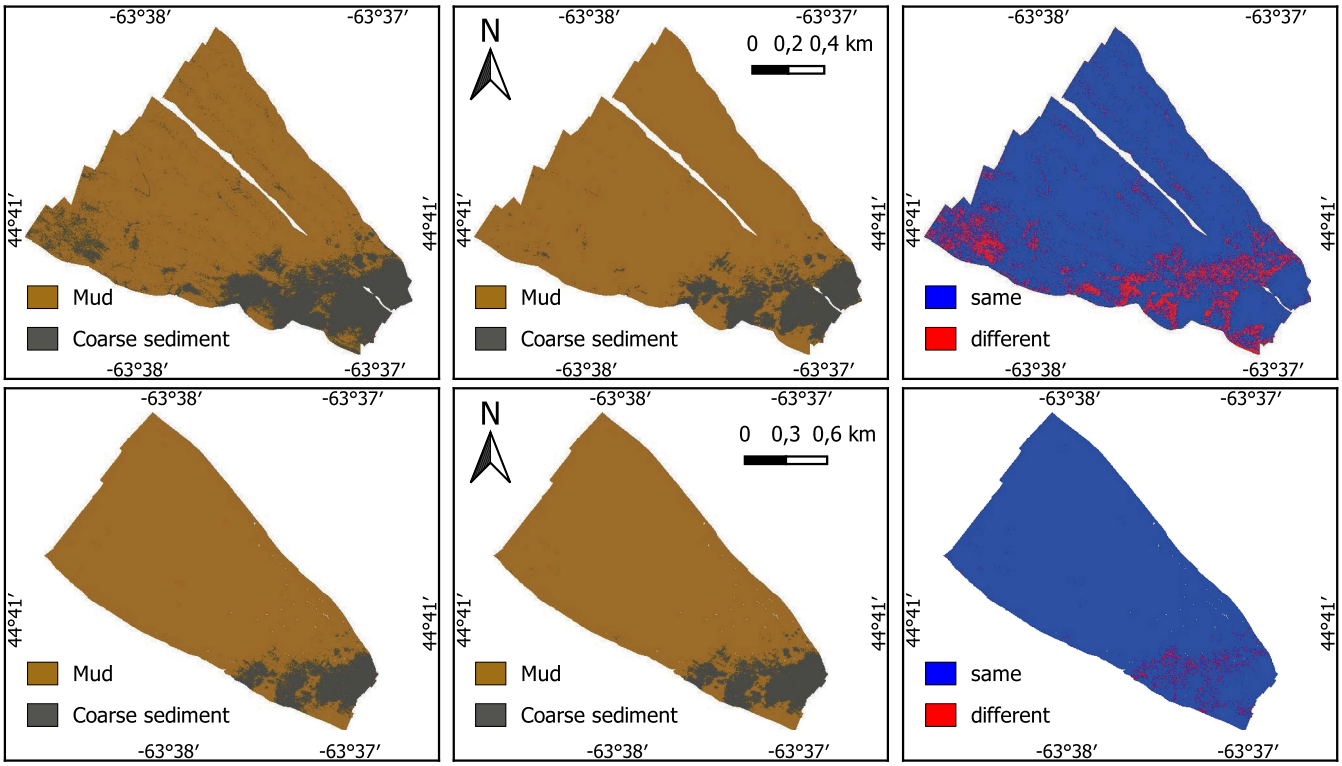

Fig. 8. Left: Classifications maps of Bedford Basin 2016 (top) and 2017 (bottom) surveys, with model trained on the 2018 survey data. Middle: Reference classification maps from models trained on the same survey data. Right: Differences.

TABLE VI
PREDICTION ON BEDFORD BASIN 2016 (TOP) AND 2017 (BOTTOM) WITH MODEL TRAINED ON 2018 DATA USING MLP CLASSIFIER (ROWS CORRESPOND TO TRUE LABELS AND COLUMNS TO PREDICTED)

	Bedford Basin 2016			
	Mud	Coarse sediment	sum	PA
Mud	30804 (66.8%)	9163 (19.9%)	39967	77.1%
Coarse sediment	137 (0.3%)	6007 (13.0%)	6144	97.8%
sum	30941	15170	F1:	71.6%
UA	99.6%	39.6%	OA:	79.8%
	Bedford Basin 2017			
	Mud	Coarse sediment	sum	PA
Mud	51670 (87.4%)	1282 (2.2%)	52952	97.6%
Coarse sediment	1361 (2.3%)	4783 (8.1%)	6144	77.9%
sum	53031	6065	f1:	87.9%
UA	97.4%	78.9%	OA:	95.5%

Bedford Basin 2016 survey are presented in Fig. 9. We observe that all models have similar performance with MLP slightly outperforming the other two methods both with respect to accuracy and F1 score. We also observe that both the bathymetry and the use of positional encoding in some cases improve while in others negatively affect the classification performance. This is also the case for BPI, however in the case of Portsmouth it did not provide valid results as it was always constant. The qualitative evaluation shows that in the case of RF classifiers, additional data sources introduce pronounced artifacts in the classification maps, which are not evident from the quantitative results. MLP on the other hand, seems to handle better these additional data sources. Even when backscatter alone are considered, MLP produces more spatially coherent results with respect to the RF model. This is also one of the reasons MLP has been considered as the reference model, besides its marginally better quantitative results.

In Table VIII, we examine how the classification performance is affected (in terms of OA and F1) as the training/validation split proportion changes, for MLP classifier. We note that the performance is not heavily affected by the splitting ratio. This is encouraging as it suggests that fewer reference data can be used for training without largely affecting the performance accuracy.

Regarding data normalization, we consider the case of model transferability where the effect of performing normalization is more evident. Considering the transferability of the model trained on Bedford Basin 2016, Table IX shows how classification performance is affected for different types of data normalization. We note that normalization increases the classification performance in all cases.

TABLE VII
EFFECT OF BATHYMETRY AND POSITIONAL ENCODING FOR DIFFERENT CLASSIFIERS (BEST VALUES APPEAR IN BOLD)

		Bedford 2016		Bedford 2017		Bedford 2018		Patricia Bay		Portsmouth		region average	
		OA (%)	F1 (%)	OA (%)	F1 (%)	OA (%)	F1 (%)	OA (%)	F1 (%)	OA (%)	F1 (%)	OA (%)	F1 (%)
RF	only BS	92.6	73.1	95.6	73.3	97.0	90.6	99.6	99.3	99.2	99.2	96.8	87.1
	with Bath.	91.7	66.9	91.9	67.5	**99.4**	**98.0**	99.9	99.9	83.2	77.7	93.2	82.0
	with BPI	92.7	72.6	95.4	73.0	96.8	90.5	98.6	97.7	-	-		
	with PE	91.2	66.7	**97.1**	**87.7**	95.2	82.8	89.1	83.7	**100**	**100**	94.5	84.2
MLP	only BS	93.0	78.6	95.2	71.2	98.5	95.8	**100**	**100**	**100**	**100**	**97.3**	**89.1**
	with Bath.	94.3	82.6	95.3	71.5	97.9	93.7	99.9	99.9	98.2	98.2	97.0	**89.1**
	with BPI	92.7	77.9	95.5	69.2	96.3	85.6	99.5	99.2	-	-		
	with PE	92.4	75.7	96.0	84.6	96.4	88.6	92.0	84.0	**100**	**100**	95.3	86.6
SVM	only BS	94.0	81.4	94.8	72.7	97.3	90.3	95.7	92.1	**100**	**100**	96.4	87.3
	with Bath.	**95.1**	**83.9**	95.0	73.2	97.1	90.2	95.3	92.0	**100**	**100**	96.5	87.9
	with BPI	94.0	81.4	94.8	72.7	97.3	90.3	95.7	92.1	-	-		
	with PE	93.1	77.9	93.6	81.2	95.4	85.1	94.1	91.6	**100**	**100**	95.2	87.2

Best values appear in bold

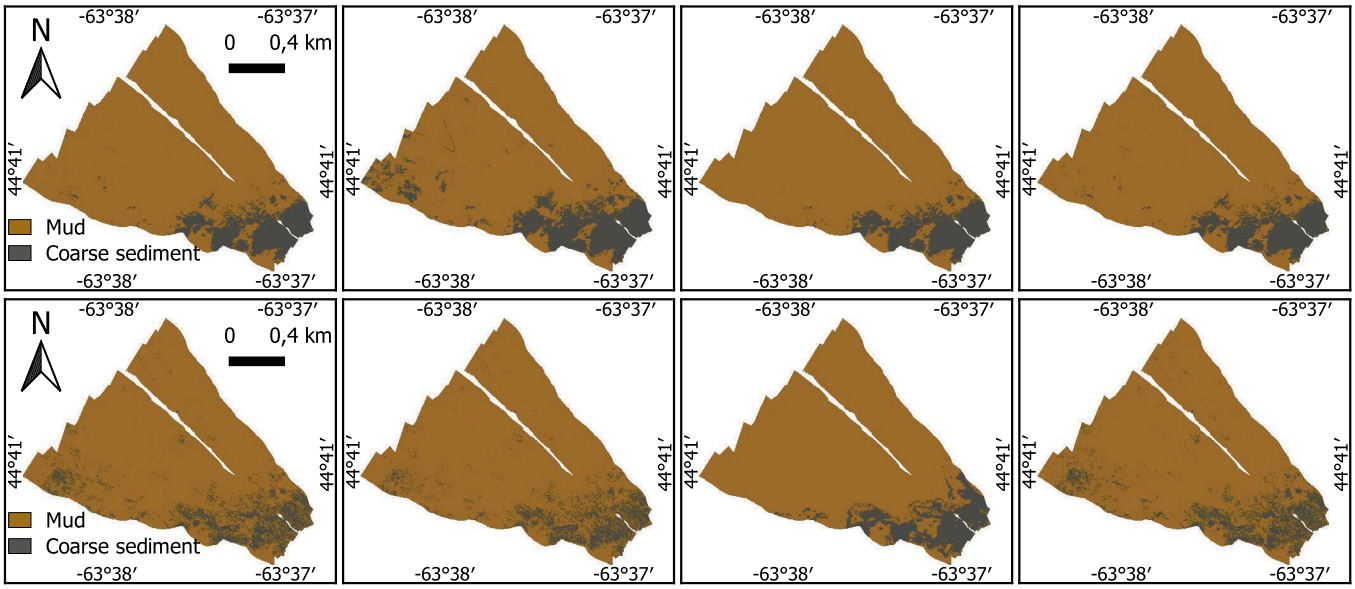

Fig. 9. Comparison of classification maps on the Bedford Basin 2016 survey data considering different data sources. 1st column: Only backscatter, 2nd col.: positional encoding, 3rd col.: bathymetry, 4th col.: BPI. The 1st row shows the results of the MLP model and the 2nd row from the RF model.

TABLE VIII
EFFECT OF DIFFERENT TRAINING/VALIDATION SPLIT PERCENTAGES (BEST VALUES APPEAR IN BOLD)

	Bedford 2016		Bedford 2017		Bedford 2018		Patricia Bay		Portsmouth		region average	
	OA (%)	F1 (%)	OA (%)	F1 (%)	OA (%)	F1 (%)	OA (%)	F1 (%)	OA (%)	F1 (%)	OA (%)	F1 (%)
30/70	94.5	88.0	95.5	86.7	91.7	73.9	96.1	94.8	100	100	95.6	88.7
50/50	**94.9**	**89.6**	**96.1**	**89.0**	95.3	90.0	98.3	97.4	100	100	96.9	**93.2**
70/30	93.3	80.5	95.3	73.7	**98.7**	**96.3**	**100**	**100**	100	100	**97.5**	90.1

Best values appear in bold

We also study the effect on the results of the size of the disk around the samples where ground truth is defined, as well as the size of the MLP hidden layers. The top panel of Fig. 10 shows how the size of the disk affects the classification accuracy. We see that for most regions a disk of size 4 m gives the best results. Nevertheless, the accuracy is relatively insensitive to the size of the disk, for the range considered. The right panel of Fig. 10 shows how the size of the neural network (number of neurons in the hidden layer) affects the classification accuracy. We note that a size of 512 gives the best results, which are

TABLE IX
DATA NORMALIZATION EFFECT USING BEDFORD 2016 AS TRAINING SET

	Bedford 2017		Bedford 2018	
	OA (%)	F1 (%)	OA (%)	F1 (%)
w/o normalization	89.6	47.3	86.4	46.3
mean/std	94.4	79.9	88.7	61.9

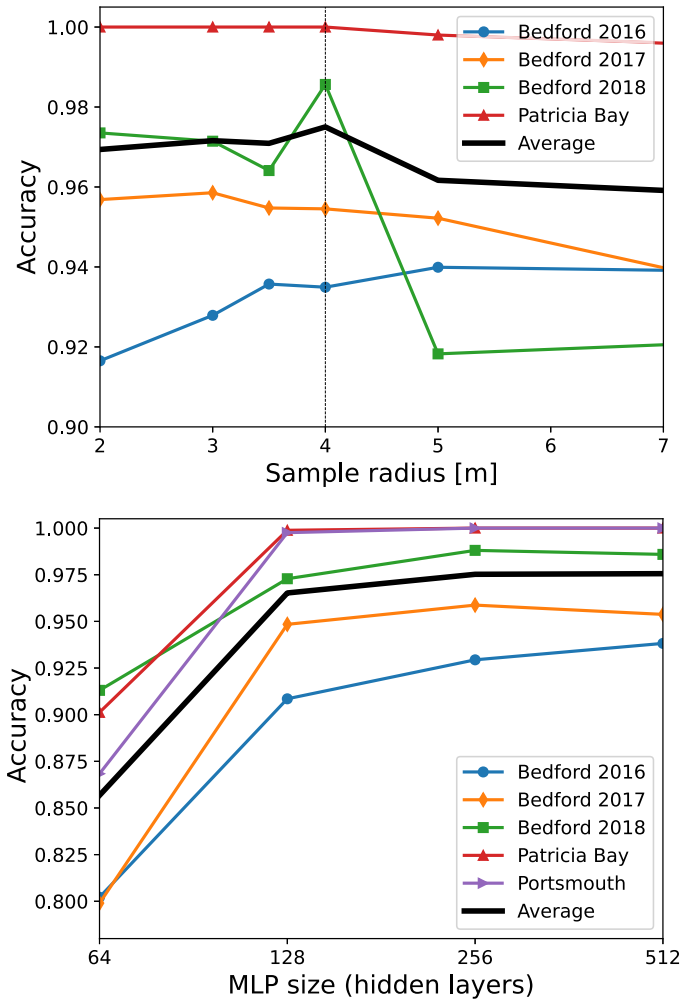

Fig. 10. Ablation with respect to the size of the disks defining ground truth top and the size of the MLP hidden layers bottom.

only marginally better though with respect to a network with size 256.

E. Discussion

Based on the ablative study performed, we note that all models achieve similar accuracy, with MLP being marginally better in average. Between RF and MLP, RFs require much less time both for training and inference with respect to MLPs, hence, they may be preferred in applications where classification efficiency is important. Still the qualitative differences in the produced maps (see Fig. 9) should be also taken into account. It is worth noting that the in the context of the literature on seabed classification from single-frequency MBES data, RF models are often found to perform better than other methods.

Moreover, it is interesting to see that the bathymetry does not always lead to improvement in the classification accuracy. This is probably because spatially disjoint training and validation sets were considered, hence the models appear to not be able to exploit the spatial correlation between backscatter data and bathymetry. We have also considered positional encoding for explicitly adding information regarding the relative location of the input data. The results confirm that positional encoding is also able to increase the model performance to a similar extent as bathymetry does, while being region-agnostic. Caution is needed though, as these additional data layers can result into artifacts in the classification map, as it can be seen in Fig. 9.

As far as comparison with other seabed classification methods based on MS-MBES survey data is concerned, we note that the methods largely diverge in the assumptions made and the way the available data are interpreted to form the seabed classes. This is reflected also on how reference data are collected and grouped as to be used for the classification process. This makes it nearly impossible to directly compare the results of these methods. The work of [16] is probably one of the few we can compare with. In these regards, although the classes considered for the Patricia Bay and Bedford Basin regions are not exactly the same, comparison of the overall accuracy results suggest that both methods can achieve very high classification performance. In fact, our method achieves higher OA for Patricia Bay 100% with respect to 91%, though not sharing the same training and validation sets, and comparable OA for the 2016 survey of Bedford Basin (98.7% with respect to 99.5%).

V. UW-MAP SERVICE

Based on the quite promising experimental results regarding the models' transferability, we have developed three models offered via a freely accessible web service available at https://uw-map.neanias.eu. Fig. 11 presents the user interface of the web service. To test the models, the service offers the multispectral images corresponding to the Lower Portsmouth Harbor 2017, the Patricia Bay 2016, and the Bedford Basin 2017 surveys. Most importantly though, the user can upload his/her own MS-MBES data to test the available models.

The models offered in the current version of the service are: 1) a model trained on all classes of the Bedford Basin regions; 2) a model trained on the classes of the Portsmouth Harbor; 3) a model trained on the classes of Patricia Bay; and 4) a model based on all classes considered here. Fig. 12 shows the results view presented to the user after running an indicative classification task on the Patricia Bay data with the three classes model. The service offers the possibility to download the georeferenced classification map in GeoTiff format.

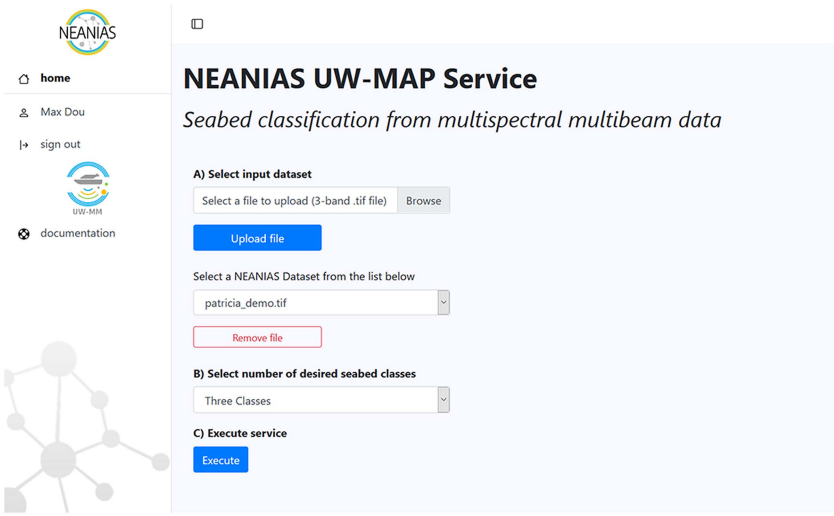

Fig. 11. User interface of the developed UW-MAP service.

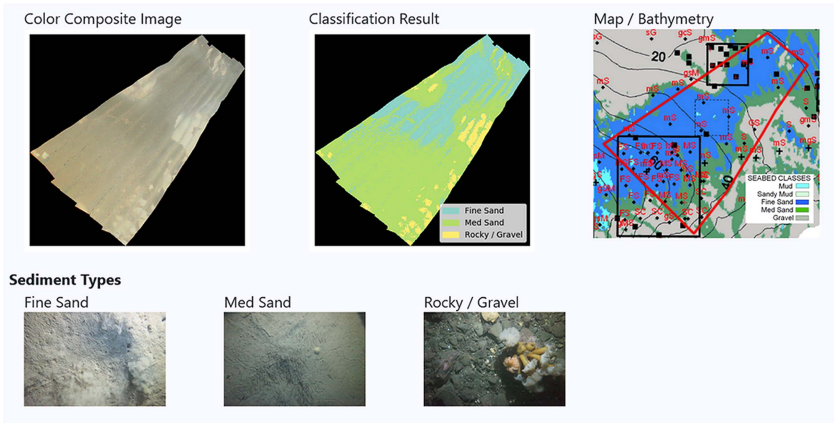

Fig. 12. Indicative UW-MAP service results view.

VI. Conclusion

We presented an end-to-end methodology for seabed classification from multispectral multibeam echosounder data. Considering five surveys made available by the R2Sonic Multispectral Challenge 2017 we show that the proposed method produces high quality classification maps, based on the backscatter data alone. Classification is performed using standard classifier models acting on region-wide multispectral images build from the per survey line acquisition data and we define reference data based on seabed grab samples. We also assess the effect of additional information provided from bathymetry and other bathymetry derived products, and propose positional encoding as an alternative way to increase spatial coherence of the result.

We make available the source code used for seabed classification on GitHub[3] together with the multispectral images and the ground-truth data used in this work. Additionally, we offer a web service building on the proposed method,[4] serving different seabed classification models for the community to assess and build upon.

[3][Online]. Available: https://github.com/mdouskos/seabed-classification
[4][Online]. Available: https://uw-map.neanias.eu/

Acknowledgment

The authors would like thank the anonymous reviewers for their thorough evaluation of our manuscript and for their constructive feedback, which lead to a substantial improvement of this work. All backscatter data were provided by R2Sonic, LLC (Austin, TX, USA) for the 2017 Multispectral Challenge. We gratefully acknowledge the support of NVIDIA Corporation with the donation of the GPUs used for this research.

References

[1] C. J. Brown and P. Blondel, "Developments in the application of multibeam sonar backscatter for seafloor habitat mapping," *Appl. Acoust.*, vol. 70, pp. 1242–1247, 2009.
[2] G. Cochrane and K. Lafferty, "Use of acoustic classification of sidescan sonar data for mapping benthic habitat in the Northern Channel Islands, California," *Continental Shelf Res.*, vol. 22, pp. 683–690, 2002.
[3] C. Brown, J. Beaudoin, M. Brissette, and V. Gazzola, "Multispectral multibeam echo sounder backscatter as a tool for improved seafloor characterization," *Geosciences*, vol. 9, 2019, Art. no. 126.
[4] T. C. Gaida, T. A. van Dijk, M. Snellen, T. Vermaas, C. Mesdag, and D. G. Simons, "Monitoring underwater nourishments using multibeam bathymetric and backscatter time series," *Coastal Eng.*, vol. 158, 2020, Art. no. 103666.
[5] J. T. Anderson, D. Van Holliday, R. Kloser, D. G. Reid, and Y. Simard, "Acoustic seabed classification: Current practice and future directions," *ICES J. Mar. Sci.*, vol. 65, no. 6, pp. 1004–1011, 2008.

[6] J. Penrose et al., "Acoustic techniques for seabed classification," Cooperative Res. Centre Coastal Zone Estuary and Waterway Management, Techn. Rep. 32, Jun. 2006.
[7] X. Ji, B. Yang, and Q. Tang, "Seabed sediment classification using multibeam backscatter data based on the selecting optimal random forest model," *Appl. Acoust.*, vol. 167, 2020, Art. no. 107387.
[8] V. Lecours, V. Lucieer, M. Dolan, and A. Micallef, *An Ocean of Possibilities: Applications and Challenges of Marine Geomorphometry*. Poznań, Poland: Int. Soc. Geomorphometry, Jun. 2015, pp. 23–26.
[9] B. Misiuk, M. Lacharité, and C. J. Brown, "Assessing the use of harmonized multisource backscatter data for thematic benthic habitat mapping," *Sci. Remote Sens.*, vol. 3, 2021, Art. no. 100015.
[10] D. Ierodiaconou et al., "Combining pixel and object based image analysis of ultra-high resolution multibeam bathymetry and backscatter for habitat mapping in shallow marine waters," *Mar. Geophys, Res.*, vol. 39, no. 1, pp. 271–288, 2018.
[11] B. Misiuk, M. Diesing, A. Aitken, C. J. Brown, E. N. Edinger, and T. Bell, "A spatially explicit comparison of quantitative and categorical modelling approaches for mapping seabed sediments using random forest," *Geosciences*, vol. 9, no. 6, 2019, Art. no. 254.
[12] A. N. Ivakin and J.-P. Sessarego, "High frequency broad band scattering from water-saturated granular sediments: Scaling effects," *J. Acoust. Soc. Amer.*, vol. 122, no. 5, pp. EL165–EL171, Nov. 2007.
[13] R. J. Urick, "The backscattering of sound from a harbor bottom," *J. Acoust. Soc. Amer.*, vol. 26, no. 2, pp. 231–235, 1954.
[14] L. Janowski, K. Trzcinska, J. Tegowski, A. Kruss, M. Rucinska-Zjadacz, and P. Pocwiardowski, "Nearshore benthic habitat mapping based on multi-frequency, multibeam echosounder data using a combined object-based approach: A case study from the rowy site in the southern baltic sea," *Remote Sens.*, vol. 10, no. 12, 2018, Art. no. 1983.
[15] T. C. Gaida, T. A. Tengku Ali, M. Snellen, A. Amiri-Simkooei, T. A. G. P. Van Dijk, and D. G. Simons, "A multispectral Bayesian classification method for increased acoustic discrimination of seabed sediments using multi-frequency multibeam backscatter data," *Geosciences*, vol. 8, no. 12, 2018, Art. no. 455.
[16] D. Buscombe and P. E. Grams, "Probabilistic substrate classification with multispectral acoustic backscatter: A comparison of discriminative and generative models," *Geosciences*, vol. 8, no. 11, 2018, Art. no. 395.
[17] B. Costa, "Mapping marine habitats using machine learning and multispectral multibeam data," NOAA Nat. Centers Coastal Ocean Sci, Tech. Rep., pp. 1–24, 2018. [Online]. Available: https://www.r2sonic.com/wp-content/uploads/2020/03/NOAA-NCCOS-Mapping-Marine-Habitats-using-Machine-Learning-and-Multispectral-Multibeam-Data.pdf
[18] R2Sonic, "R2sonic challenges," 2017. [Online]. Available: https://www.r2sonic.com/resources/challenges/
[19] C. J. Brown, S. J. Smith, P. Lawton, and J. T. Anderson, "Benthic habitat mapping: A review of progress towards improved understanding of the spatial ecology of the seafloor using acoustic techniques," *Estuarine, Coastal Shelf Sci.*, vol. 92, no. 3, pp. 502–520, 2011.
[20] E. R. Lundblad et al., "A benthic terrain classification scheme for American Samoa," *Mar. Geodesy*, vol. 29, no. 2, pp. 89–111, 2006.
[21] D. R. Jackson and M. D. Richardson, *High-Frequency Seafloor Acoustics*. New York, NY, USA: Springer, 2007, pp. 171–200.
[22] P. Mertikas and K. Karantzalos, "Seafloor mapping from multispectral multibeam acoustic data at the European open science cloud," *Int. Arch. Photogrammetry, Remote Sens. Spatial Inf. Sci.*, vol. 43, no. B2, pp. 985–990, 2020.
[23] D. W. Caress, D. N. Chayes, and C. dos Santos Ferreira, "Seafloor mapping software: Processing and display of swath sonar data," 2016. [Online]. Available: https://www3.mbari.org/data/mbsystem/index_ldeo.html
[24] D. W. Caress and D. N. Chayes, "New software for processing sidescan data from sidescan-capable multibeam sonars," in *Proc. Conf. 'Challenges Changing Glob. Environ.'*, 1995, vol. 2, pp. 997–1000.
[25] D. W. Caress and D. N. Chayes, "Improved processing of hydrosweep DS multibeam data on the R/V maurice ewing," *Mar. Geophys. Res.*, vol. 18, no. 6, pp. 631–650, 1996.
[26] R. E. Francois and G. R. Garrison, "Sound absorption based on ocean measurements: Part I: Pure water and magnesium sulfate contributions," *J. Acoust. Soc. Amer.*, vol. 72, no. 3, pp. 896–907, 1982.
[27] A. C. G. Schimel et al., "Multibeam sonar backscatter data processing," *Mar. Geophys. Res.*, vol. 39, no. 6, pp. 121–137, 2018.
[28] A. Telea, "An image inpainting technique based on the fast marching method," *J. Graph. Tools*, vol. 9, pp. 23–34, 2004.
[29] M. Bertalmio, A. L. Bertozzi, and G. Sapiro, "Navier-stokes, fluid dynamics, and image and video inpainting," in *Proc. IEEE Conf. Comput. Vis. Pattern Recognit.*, 2001, pp. 1–9.
[30] D. Ulyanov, A. Vedaldi, and V. Lempitsky, "Deep image prior," in *Proc. IEEE Conf. Comput. Vis. pattern Recognit.*, 2018, pp. 9446–9454.
[31] L. Breiman, "Random forests," *Mach. Learn.*, vol. 45, no. 1, pp. 5–32, 2001.
[32] I. Goodfellow, Y. Bengio, A. Courville, and Y. Bengio, "Deep feedforward networks," in *Deep Learning*. Cambridge, MA, USA: MIT Press, ch. 6, 2016.
[33] C. Cortes and V. Vapnik, "Support-vector networks," *Mach. Learn.*, vol. 20, no. 3, pp. 273–297, 1995.
[34] H. Meyer, C. Reudenbach, S. Wöllauer, and T. Nauss, "Importance of spatial predictor variable selection in machine learning applications — moving from data reproduction to spatial prediction," *Ecological Model.*, vol. 411, Nov. 2019, Art. no. 1088152019.
[35] C. Karakizi, I. Tsiotas, Z. Kandylakis, A. Vaiopoulos, and K. Karantzalos, "Assessing the contribution of spectral and temporal features for annual land cover and crop type mapping," *Int. Arch. Photogrammetry, Remote Sens. Spatial Inf. Sci.*, vol. 43, no. B3, pp. 1555–1562, 2020.
[36] A. Vaswani et al., "Attention is all you need," in *Proc. Int. Conf. Adv. Neural Inf. Process. Syst.*, 2017, pp. 5998–6008.
[37] M. Tancik et al., "Fourier features let networks learn high frequency functions in low dimensional domains," in *Proc. Int. Conf. Adv. Neural Inf. Process. Syst.*, 2020, vol. 33, pp. 7537–7547.
[38] Leidos Corporation, "Gsflib, the generic sensor format library," 2014. [Online]. Available: https://www3.mbari.org/data/mbsystem/formatdoc/GSF/GSF_lib_03-05.pdf
[39] A. M. Kaskela et al., "Picking up the pieces—harmonising and collating seabed substrate data for European maritime areas," *Geosciences*, vol. 9, no. 2, 2019, Art. no. 84.
[40] B. Biffard, S. Bloomer, R. Chapman, J. Preston, and J. Galloway, "Single-beam seabed characterization: A test-bed for controlled experiments," in *Proc. Eur. Conf. Underwater Acoust.*, 2006, pp. 12–15.
[41] B. R. Biffard, "Seabed remote sensing by single-beam echosounder: Models, methods and applications," Ph.D. dissertation, Sch. Earth Ocean Sci., Univ. Victoria, Victoria, BC, Canada, 2011.
[42] T. C. Weber and L. G. Ward, "Observations of backscatter from sand and gravel seafloors between 170 and 250 kHz," *J. Acoust. Soc. Amer.*, vol. 138, no. 4, pp. 2169–2180, Oct. 2015.
[43] J. Heaton, G. Rice, and T. Weber, "An extended surface target for high-frequency multibeam echo sounder calibration," *J. Acoust. Soc. Amer.*, vol. 141, no. 4, pp. EL388–EL394, 2017.

Valsamis Ntouskos received the engineering diploma from the School of Rural and Surveying Engineering, National Technical University of Athens (NTUA), Athens, Greece, in 2006, the B.Sc. degree in electronics engineering in 2010, the M.S.E. degree in artificial intelligence and robotics in 2012, and the Ph.D. degree in computer engineering with honors in 2016 from the Sapienza University of Rome, Sapienza, Italy, working on "Inverse Problems Theory in Shape and Action Modeling."

From 2017 to 2020, he was Researcher with the Department of Computer, Control, and Management Engineering, Sapienza University of Rome. As of 2020, he is a Research Fellow with the Remote Sensing Lab, NTUA. He has several publications in top-tier international conferences and journals in the fields of machine learning and computer Vision. His teaching and research interests include computer vision, remote sensing, machine learning and robotics, focusing on the design and development of autonomous perception and nonconventional imaging systems.

Dr. Ntouskos serves as a Program Committee Member and reviewer for top rank international conferences and journals of his field. He has participated in several EU funded Research and Innovation projects on topics related to robotics and ICT.

Panagiotis Mertikas received the integrated master's degree in rural surveying engineering in 2018 from the National Technical University of Athens (NTUA), Athens, Greece, where he is currently working toward the postgraduate degree in "marine technology and science" an interdisciplinary postgraduate study program.

His research interests include applications of marine technology in environmental monitoring and management, remote sensing techniques for coastal and oceanic studies, geospatial analysis, and mapping for marine spatial planning.

Angelos Mallios (Member, IEEE) received the Ph.D. degree in robotics from Universitat de Girona, Girona, Spain, in 2014.

He is the Cofounder of PLOATECH and has been holding visiting appointments with Wood Hole Oceanographic Institution from 2006 to 2020. He has been in marine research since 1999, where he has served as a diving and ROV supervisor, been responsible for the maintenance of the manned submersible THETIS with the Hellenic Center for Marine Research (HCMR), and he has participated in a number of research cruises. Angelos's research interests include the design and autonomy of underwater vehicles and oceanography sensory technology.

Dr. Mallios has received a number of awards, including three Marie Skłodowska-Curie Actions, first and second places in two Student Autonomous Underwater Challenge, and Best Poster Award at OCEANS 2011.

Konstantinos Karantzalos (Senior Member, IEEE) received the engineering diploma from the National Technical University of Athens, (NTUA), Athens, Greece, in 2000, and the Ph.D. degree from SRSE, NTUA in collaboration with Ecole Nationale de Ponts et Chaussees CERTIS/Imagine, ENPC, Paris, France, in 2007.

In 2007, he joined the Department of Applied Mathematics, Ecole Centrale de Paris, Gif-sur-Yvette, France, as a Postdoctoral Researcher. He is currently a Professor with the National Technical University of Athens, joining the Remote Sensing Laboratory (RSLab), School of Rural, Surveying, and Geo-Informatics Engineering. He is also occasionally affiliated with the Institute of Communications and Computer Systems (ICCS) and the Athena Research Center. He has numerous publications in international journals and conferences and a number of awards and honors for his research contributions. He has 19 years of research experience, while being involved with more than 28 EU and national excellence/competitive research projects as a Principal investigator and as a Researcher towards the design, development, and validation of state-of-the-art methodologies and cutting-edge technology in geomatics, earth observation, and computer vision. His teaching and research interests include earth observation and remote sensing, geospatial Big Data and analytics, computer vision and machine learning, environmental monitoring, and precision agriculture.

Dr. Karantzalos serves as a Scientific/Program Committee Member at international conferences and as a reviewer in top-rank international journals